

INS-Aided Odometry and Laser Scanning Data Integration for Real Time Positioning and Map-Building of Skid-Steered Vehicles

G. Anousaki^a, V. Gikas^{b*}, K. Kyriakopoulos^a

^a School of Mechanical Engineering, Control System Laboratory, National Technical University of Athens, 9 H. Polytechniou St., Zographos, Athens, 15780, Greece – anousaki@mail.ntua.gr

^b School of Rural and Surveying Engineering, General Geodesy Laboratory, National Technical University of Athens, 9 H. Polytechniou St., Zographos, Athens, 15780, Greece – vgikas@central.ntua.gr

Commission V

KEY WORDS: mobile robots, map-building, skid steered vehicles.

ABSTRACT:

An enhanced odometry method coupled with an inertial navigation sensor is introduced for skid-steered vehicle positioning in outdoor environments. In the proposed scheme, robot positioning and attitude is estimated based on an experimentally derived kinematic model. Besides, a low-cost INS unit is used to improve the quality of the rotational velocity of the robot as it is obtained by differential odometry. It is concluded that a reliable positioning can be derived with the use of a comprehensive DIA procedure for outlier removal and the fusion of odometry with inertial data through a discrete Kalman filter. The map-building component of the system is based on the integration of a pair of high sensitivity 2D laser scanners suitably mounted on the vehicle. Finally, an optimum estimate of the robot position and attitude is derived through data fusion of the dead-reckoning and map-matching information. The technique has been implemented on-board an experimental skid-steered vehicle in cases of extreme motion, including runs with steep turns and variable velocity.

1. INTRODUCTION

Reliable positioning is an essential component of any autonomous vehicle system. In the case of a moving robot the navigation problem is usually termed as Simultaneous Localization and Mapping (SLAM). In this problem, the mobile robot starts in an unknown position in an unknown environment and proceeds to incrementally build a navigation map of its surroundings while simultaneously use this map to update its position (Nebot, 2002; Bayout 2006). There have been several applications of this technology in a number of different environments such as indoors, underwater and outdoors. This study focuses in the semi-structured outdoor environment. Known problems encountered in this environment relate to the fact that the ground surface is rarely clean and the distances and velocities are of higher order compared to the ones found indoors. The surroundings are often not well defined and there are limitations imposed by topography and vegetation. Most of the existing work in outdoor environments is based on the use of Extended Kalman Filter. In this approach, the inherent state vector in most algorithms consists of the vehicle states (robot position and orientation) as well as of the feature states (point positions). The downside of this generalized approach lies in the large number of system states. As the number of features grows with the area of operation, the standard filter computation becomes impracticable for real time applications.

In this study, an alternative positioning and map-building methodology appropriate for skid-steered mobile robots is introduced. Skid steered vehicles differ from explicit steering ones in the way that they turn. The lack of steering wheel

results in navigation that is determined by the speed change in either side of the skid steering vehicle. As a result, terrain irregularities may cause unpredictable power requirements which, in turn, affect the kinematics of the vehicle (Doitsidis et al, 2002; Tao et al, 1999). The navigation technique adopted in this study relies on dead-reckoning data derived by differential odometry and an inertial sensor as well as laser scanning observations. As opposed to other techniques, the feature states are defined in the form of line segments – and thus, the number of states in the system is reduced which, in turn, makes the computational algorithm more efficient in the large scale environment. The observations are fused using a modified Kalman filter that is based on the covariance intersection approach. In this manner the computational steps are simple and fast, whereas the disadvantage of processing uncorrelated observations is mitigated. The proposed method is assessed with real data collected for a number of field experiments.

2. PROBLEM FORMULATION

The proposed algorithm works iteratively in a number of sequentially applied steps according to the layout diagram shown in Figure 1. A first estimate of the robot's position comes from fusion based integration using wheel-encoder and inertial data. Next, a local visible map attached to the robot coordinate system is constructed based on laser scanning readings. This information is coupled with the robot position to produce a visible global map of the vehicle's surroundings. As no absolute positioning systems assumed in this study, the global map refers to an arbitrary chosen space coordinate system – i.e., it does not relate to an earth centered earth fixed

* Corresponding author

or map projection coordinate system. Through map feature association between the currently visible portion of the global map and the global map obtained from previous iterations, a second estimate of the robot's position is computed. Finally, based on this estimate and the data from dead-reckoning an improved location of the robot and an updated version of the global map is produced based on the covariance intersection data filtering technique.

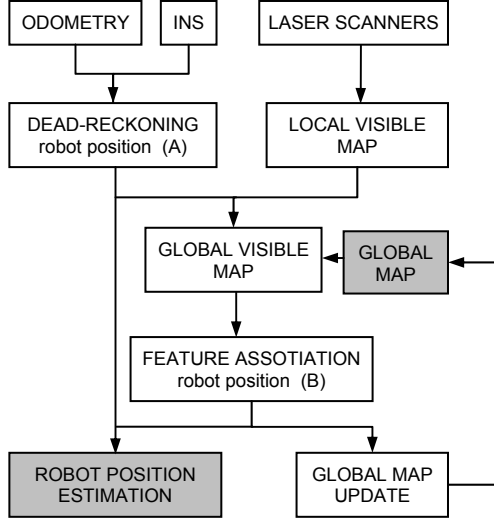


Figure 1. Proposed SLAM processing scheme

2.1 Robot's Positioning Based on Dead Reckoning

2.1.1 Differential odometry: In the case of explicit steering vehicles a differential odometer allows to derive distance and direction information from which the kinematics of the vehicle can be computed. With v_r and v_l denoting the velocities measured by the right and left wheel encoders, the linear velocities u_x , u_y and the angular velocity ω_{ODO} are given by (Hofmann-wellenhof, 2003):

$$\begin{bmatrix} u_x & u_y & \omega_{ODO} \end{bmatrix}^T = \begin{bmatrix} 0 & \frac{v_r + v_l}{2} & \frac{v_r - v_l}{2} \end{bmatrix}^T \quad (1)$$

where l is the wheel separation (Figure 2). In the case of skid steering, the motion is achieved by creating a differential thrust between the two sides of the vehicle – and thus, Equation 1 is not explicitly applicable. To cope with this fact an experimentally derived kinematic model was adopted for the purpose of this study. More specifically, a terrain-dependent relation between the linear and angular velocity of the robot and the velocities observed on the two sides of the vehicle was determined through extensive experiments on various terrains. For this purpose, a specially constructed trailer system was used to measure the linear and angular velocity of the robot for different trajectories. The elements of matrix A that relates these velocity expressions for a specific type of terrain were computed based on linear regression analysis [Kyriakopoulos and Anousaki, 2004]. In algebraic notation the experimental kinematic model stands as:

$$u_{ODO} = A v_{ODO} \quad (2)$$

$$\text{with } u_{ODO} = \begin{bmatrix} u_x & u_y & \omega_{ODO} \end{bmatrix}^T, \quad v_{ODO} = \begin{bmatrix} v_r & u_l \end{bmatrix}^T$$

2.1.2 Inertial positioning: Since in this study it is assumed that absolute positioning (such that provided by GPS or other GNSS systems) is unavailable, a low cost inertial unit was used to aid robot odometry. This system provides a complete suite of tri-axial accelerations and angular velocities. However, due to the low dynamics associated with the robot performance and other factors relating to temperature induced bias, only the yaw angular velocity measurements were utilized. More specifically, this type of low latency dynamic information was proved particularly useful where the wheel encoders failed. A detailed analysis of the preliminary tests, the problems and the results concerned with the use of the INS system in this study are given in (Kyriakopoulos and Anousaki, 2004).

2.1.3 Fusion Based Integration: A first estimate of the robot position is obtained by integrating odometry with inertial data by means of a Kalman filter. In effect, dead-reckoning results in the following information for the robot kinematics:

$$u_{ODO} = A \begin{bmatrix} v_r & v_l \end{bmatrix}^T \quad (3)$$

$$u_{INS} = \begin{bmatrix} \int a_x & \int a_y & \omega_{INS} \end{bmatrix}^T \doteq \begin{bmatrix} \omega_{INS} \end{bmatrix} \quad (4)$$

It is assumed that these two estimates exhibit a Gaussian character. However, their correlations are unknown and hence the Covariance Intersection (CI) filtering scheme is used for fusing the observations (Uhlmann and Julier, 1997; Dissanayake et al, 2002). The CI method is a sub-optimal covariance update technique that relies on the Kalman filter principle. In fact, it provides a computationally efficient mechanism for data fusion but discards a considerable amount of information (albeit unknown) of the cross-correlations between the two robot position estimates. According to this integration scheme the velocity of the robot u_{DR} and its associated covariance matrix $C_{u_{DR}}$ is computed as follows:

$$u_{DR} = C_{u_{DR}} \left[\omega C_{u_{ODO}}^{-1} u_{ODO} + (1-\omega) C_{u_{INS}}^{-1} u_{INS} \right] \quad (5)$$

$$C_{u_{DR}} = \left[\omega C_{u_{ODO}}^{-1} + (1-\omega) C_{u_{INS}}^{-1} \right]^{-1} \quad (6)$$

In Equations 5 and 6, u_{ODO} , u_{INS} and $C_{u_{ODO}}$, $C_{u_{INS}}$ refer to the robot velocity estimates and their covariance matrices for the odometry and inertial data respectively. According to the formulation of the CI filter the parameter ω ($0 \leq \omega \leq 1$) is computed to minimize the size of the trace of the updated covariance matrix $C_{u_{DR}}$. Also, in order to improve to assure quality control the data are pre-filtered for outliers according to the equation:

$$\frac{(\omega_{INS} - \omega_{ODO})^2}{2(\sigma_{\omega_{INS}}^2 + \sigma_{\omega_{ODO}}^2)} \leq 1 \quad (7)$$

where $\sigma_{\omega_{INS}}^2$ and $\sigma_{\omega_{ODO}}^2$ are the variances of the yaw angular velocity for the wheel encoders and the inertial system. Finally, the robot position as derived from dead-reckoning is computed as follows:

$$X_{DR}(+) = X_{DR}(-) + u_{DR}(-)\delta\tau \quad (8)$$

$$C_{X_{DR}}(+) = C_{X_{DR}}(-) + \delta\tau^2 C_{u_{DR}}(-) \quad (9)$$

where (-) and (+) denote the previous and current instant state and covariance matrix estimates and $\delta\tau$ is the time step. Given the relatively low dynamic behaviour of the robot kinematics and the low operational frequency of the laser scanners a time step of ~ 0.4 sec was set to operate the Kalman filter.

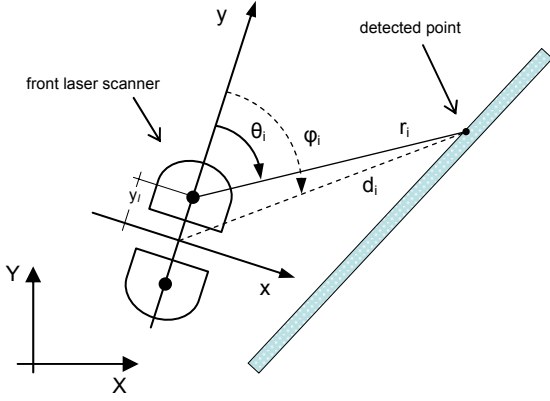


Figure 2. Laser scanning observation layout

2.2 Visible Map Construction

As pointed out in Section 1, in this study the feature states which map the robot surroundings are defined in the form of line segments. Thereby, a set of polar line parameters $l_k = [a_k, b_k]^T$, $k=1, \dots, n$ and the coordinates of their starting and ending points $[x_k, y_k]_{start}^T, [x_k, y_k]_{end}^T$ are computed in the robot coordinate frame. This is performed in three subsequent steps. Firstly, the feature coordinates $[x_i, y_i]^T$ for every observed point i are computed using the laser scanner raw observations. As shown in Figure 2, the observed directions θ_i and distances r_i are reduced to their respective values in the robot coordinate system φ_i and d_i as follows:

$$[x_i, y_i]^T = [d_i \sin \varphi_i, d_i \cos \varphi_i]^T \quad (10)$$

$$\varphi_i = \text{atan} \left(\frac{r_i \sin \theta_i}{r_i \cos \theta_i + y_i} \right) \quad (11)$$

$$d_i = \frac{r_i \sin \theta_i}{\sin \varphi_i} \quad (12)$$

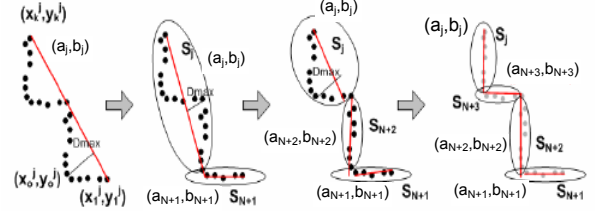


Figure 3. Processing algorithm for line segmentation

In the sequel, the feature points are grouped into clusters of points, each cluster containing a significant number of neighboring points. In mathematical terms, this separation is obtained by applying the following formula on the reduced direction and distance measurements φ_i and d_i :

$$|d_{i+1} - d_i| < d_{max} \quad |\varphi_{i+1} - \varphi_i| < \varphi_{max} \quad (13)$$

where the threshold values φ_{max} and d_{max} are set equal to 20 cm and 0.018 rads considering the robot size. At a final stage, the data points that belong to every cluster are split in a number of line segments by applying the recursive line split method depicted in Figure 3. Then, the data points that correspond to every line segment are regressed to compute the line parameters $l_k = [x_k, y_k]^T$ and their covariance matrix C_{l_k} .

2.3 Map Matching

At this stage of the process the local visible map produced at the previous computational step is transformed from the robot coordinate frame to the global map coordinate system. Coordinate systems transformation is achieved by applying a translation and a rotation on the line parameters of the local map using the robot position and orientation computed by Equation 8. Thus:

$$l_{NEW}^G = f(X_{DR}, l_{NEW}^L) \quad (14)$$

where l_{NEW}^L, l_{NEW}^G denote the line parameters observed at the current epoch, expressed at the robot and global coordinate systems respectively and X_{DR} denotes the robot states as computed from dead-reckoning. The statistical significance of the map features obtained at the current epoch l_{NEW}^G with respect to the map features obtained from previous epochs l_{FIXED}^G is assessed by applying the χ^2 distribution on the Mahalanobis distance with two degrees of freedom at 90% confidence level. This test reads as (Manly, 1994):

$$D^M = (l_{FIXED}^G - l_{NEW}^G) (C_{l_{FIXED}^G}^G + C_{l_{NEW}^G}^G)^{-1} (l_{FIXED}^G - l_{NEW}^G)^T \leq \chi^2 \quad (15)$$

This testing procedure results in a subset I of the total number of line segments k that fulfills the criterion of Equation 15. Based on this information an improved estimate of the robot position X_M is obtained by computing a translation and rotation set of parameters using the pairs of respective line parameters l_{NEW}^G and l_{FIXED}^G . This is realized by minimizing the following criterion:

$$F = \sum_{i=1}^I \left[l_{FIXED_i}^G - f(X_M, l_{NEW_i}^L) \right]^2 \quad (16)$$

2.4 Robot Positioning and Map Construction Update

In the final stage of the computing circle an improved estimate for the robot position and an updated version of the global map is computed. In a similar manner to the data fusion approach detailed in Section 2.1.3, a CI Kalman filter is used to integrate the robot position derived from dead-reckoning X_{DR} and from the map matching steps X_M . This is realized by:

$$X = C_{X_{DR}} \left(\zeta C_{X_{DR}}^{-1} X_{DR} + (1-\zeta) C_{X_M}^{-1} X_M \right) \quad (17)$$

$$C_{X_{DR}} = \left(\zeta C_{X_{DR}}^{-1} + (1-\zeta) C_{X_M}^{-1} \right)^{-1} \quad (18)$$

where ζ ($0 \leq \zeta \leq 1$) is a weighting factor that is computed to minimize the trace of the updated covariance matrix.

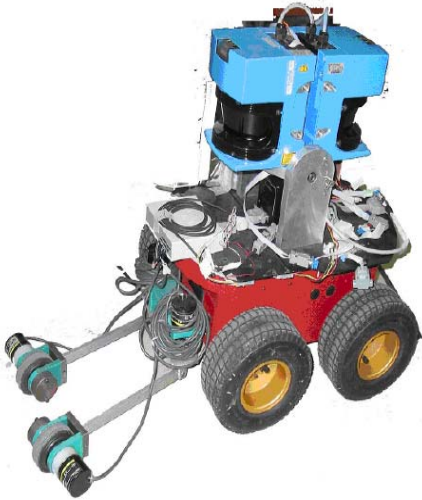


Figure 4. Experimental setup

Finally, based on the improved robot position estimate the global map is updated. The process differs for the line segments constructed in previous iterations and for those constructed for a first time in the current epoch. Previously constructed line segments are incorporated in the global map by applying Equation 14 in the improved robot position which is given by Equation 17. These, are statistically examined as explained in Section 2.3 and selectively merged in the global map. Finally, the newly constructed line segments are introduced into the global map for use in the next iteration after they have been updated by applying the improved robot position on Equation 14.

3. EXPERIMENTAL EVIDENCE

3.1 Mobile Robot and Navigation Sensors

The experimental system that was used to test the proposed algorithm is shown in Figure 4. It consists of the mobile robot Pioneer 2-AT made by Activmedia. It is a four wheel, differently steered vehicle that is primarily designed to operate in the outdoor environment. It bears two optical encoders at the front which measure the rotation of the wheels at both sides of the vehicle. Data manipulation and recording was accomplished with the help of an onboard computer provided by Octagon, running Linux. Data communication was done serially, whereas the operation of the vehicle was accomplished via a wireless LAN system.

Vehicle navigation and area mapping were performed using the robot encoders, a low cost inertial navigation sensor and the laser scanners. The inertial unit is a DMU-HDX system manufactured by Crossbow. It is based on MEMS technology and incorporates three accelerometers ($\pm 2Gs$) and three gyros (200 deg/sec). As shown in Figure 4, two SICK LMS-200 laser scanners were fixed on the top of the vehicle providing a 360 deg azimuthal coverage. They operate at 2.5 Hz, while their operational range can reach 8 m with an angle increment of 0.5 deg.

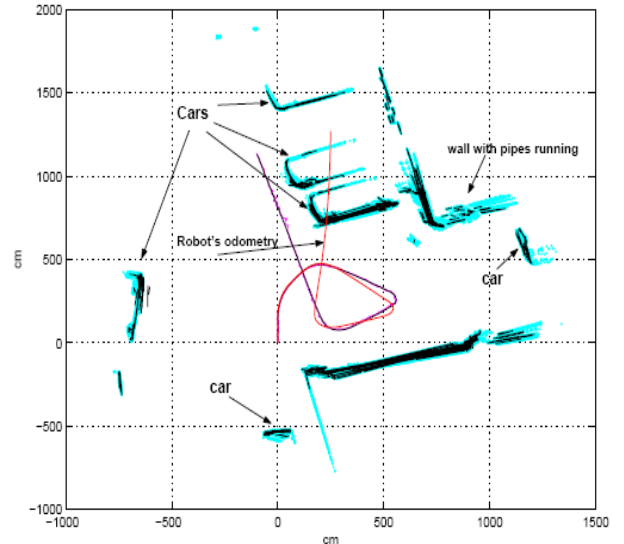


Figure 5. Robot navigation and mapping solution

3.2 Data Analysis and Results

In order to test the feasibility of the algorithm in terms of correctness and computational efficiency a number of experiments were conducted. These, include runs on different terrains and for varying trajectories. In this article only summary results are discussed for a limited number of test runs. The data were collected at a parking area featuring buildings on its surroundings. Figure 5 shows the robot navigation and mapping solution derived at the three stages of the applied algorithm – i.e., the robot odometry, the map matching and the final robot position. The first thing to note from this plot is that odometry, if used alone, deviates considerably from the actual robot path. The same conclusion is evident from the robot azimuth estimates shown in Figure 6. This phenomenon is mainly due to wheel skidding at sharp curves. Examination of Figure 5 in more detail shows that the map matching solution

produces a relatively spiky solution. This is due to the differences in the feature locations computed at subsequent epochs. However, the robot trajectory derived after the covariance intersection filtering has been applied is rather continuous and smooth. Finally, despite the fact that the map estimate is a clear representation of the robot surroundings, a large number of overlapping segments is evident. It is anticipated that, if a high pass filter is applied at the stage of line formation, a sharper outline of the map features will be produced.

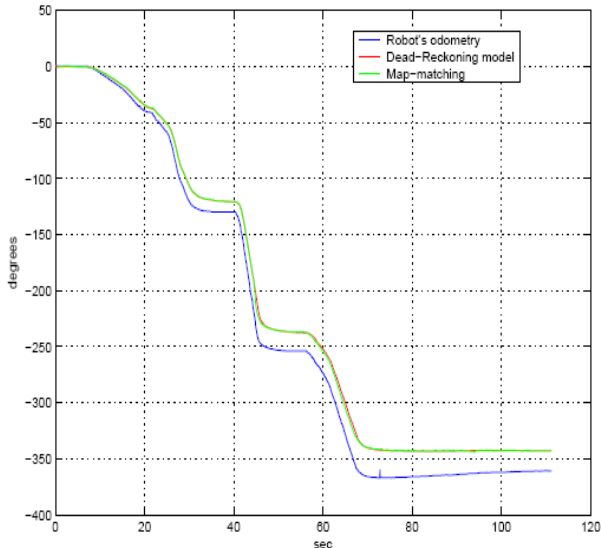


Figure 6. Robot orientation

4. CONCLUDING REMARKS

Extended tests undertaken under various terrain and robot operating conditions have shown that the system can produce satisfactory results. More specifically, the maximum errors observed in the robot navigation solution are 0.1 m and 3 deg. Also, the accuracy of the final map is of the order of 0.04 m with respect to the robot position. These figures were overall verified using conventional geodetic techniques of a higher accuracy.

REFERNCES

- Bayout, F. A., 2006. Development of a Robotic Mobile Mapping System by Vision-Aided Inertial Navigation: A Geomatics Approach, PhD Thesis, Ecole Polytechnique Federale de Lausanne, p. 183.
- Dissanayake, G., Williams, S. B., Durrant-Whyte, H., Bailey, T., 2002. Map Management for Efficient Simultaneous Localization and Mapping (SLAM), *Autonomous Robots*, 12, pp.267-286.
- Doitsidis, L., Valavanis, K. P., Tsourveloudis, N. C., 2002. Fuzzy Logic Based Software Control Architecture for a Skid Steering Vehicle, *Proceedings of the IEEE Third International Workshop on Robot Motion and Control*, Polland, pp.279-284.
- Hofmann-Wellenhof, B., Legat, K., Wieser, M., 2003. *Navigation: Principles of Positioning and Guidance*, Springer Wien New York, p. 427.

Kyriakopoulos, K. J., Anousaki, G. C., 2004. A Dead-Reckoning Scheme for Skid-Steered Vehicles in Outdoor Environments, *International Conference on Robotics and Automation*, May 2004.

Manly, B., F., J., 1994. *Multivariate Statistical Methods: A Primer*, Chapman and Hall, New York.

Nebot, E., 2002. Simultaneous Localization and Mapping, 2002 Summer School, Navigation System Design (KC-4), 31 July.

Tao, K., Takezono, S., Minamoto, H., 1999. Two-dimensional Motion of Four-Wheel Vehicles, *Vehicle Systems Dynamics*, 32, pp. 441-458.

Uhlmann, K. J., Julier, S. J., Csorba, M., 1997. Simultaneous Map Building and Localization using Covariance Intersection, *SPIE*, 37, pp 2-11.